

Nonlocal Effects in Spiral Waves

Ehud Meron

Department of Chemical Physics, Weizmann Institute of Science, Rehovot 76100, Israel
(Received 3 March 1989)

A theory of spiral waves is presented that includes nonlocal effects due to wave-front interactions. Evolution equations for the spiral wave front are derived from the basic reaction-diffusion system, using a singular perturbation method. It is shown that nonlocal effects play a crucial role in stabilizing the dynamics of spiral waves and may substantially affect their spatiotemporal behavior. In particular, conditions are found under which spiral cores expand in time. An expression for the normal velocity is derived and compared with previous results.

PACS numbers: 87.22.As, 05.45.+b, 82.40.Fp

Rotating spiral waves have been observed in a variety of chemical and biological nonequilibrium systems; oxidation waves in reactive solutions¹⁻³ and waves of electrical and neuromuscular activity in physiological systems⁴ are common examples. Early attempts to describe spiral waves employed known geometrical forms such as the involute of a circle or the Archimedean spiral.⁵ When rotated at fixed angular velocities these forms describe spiral waves whose normal velocities are constant along the spirals. It was later realized that curvature may significantly reduce the normal velocity in the vicinity of the spiral core and a better description of spiral waves, based on the velocity-curvature relationship, has been proposed.⁶ There are, however, additional effects, nonlocal in nature, that have escaped theoretical consideration: parallel portions of the spiral wave-front interact with each other during propagation.⁷ In this Letter I present a dynamical theory of spiral waves that includes both curvature and wave-front-interaction effects.

The significance of wave-front interactions follows in part from the consideration of the effect of curvature alone. Away from the spiral tip curvature acts to smooth out small perturbations.⁸ In the vicinity of the tip, on the other hand, curvature becomes a destabilizing factor: Upon straightening a small segment that contains the tip, curvature is reduced, normal velocity is enhanced, and further straightening is favored. Figure 1 illustrates these considerations. This instability causes wave-front interactions to become particularly significant: The perturbation illustrated in Fig. 1 is quenched in the presence of a wave front ahead of the tip that exerts a repulsive force. The dynamics and form of the spiral wave will be sensitive to the magnitude of that force. In the systems that have been introduced above a repulsive force originates from the refractory period that is imposed on sites at the wake of a propagating wave front.^{4,6,8}

I will be concerned here with two-dimensional homogeneous media described by reaction-diffusion equations (RDE's) of the form

$$\partial_t \mathbf{U} = \mathbf{L}\mathbf{U} + \mathbf{N}(\mathbf{U}) + D\nabla^2 \mathbf{U}, \quad (1)$$

where \mathbf{U} represents a set of fields and \mathbf{L} and \mathbf{N} are, respectively, the linear and nonlinear parts of the reaction kinetics. For the sake of simplicity all diffusion constants are assumed to be equal; thus D in (1) is a scalar. The generalization to nonequal diffusion constants is straightforward. It is also assumed that $\mathbf{N}(\mathbf{0}) = \mathbf{0}$. The solution $\mathbf{U} = \mathbf{0}$ represents the quiescent state of the medium.

It is advantageous to work in a coordinate system having a spiral structure and rotating with a fixed angular velocity. In such a frame one may expect the RDE's to decompose into an "unperturbed" part, one dimensional in a coordinate normal to the spiral, and a perturbation \mathbf{P} reflecting among other things the fact that the coordinate system is only an approximation of the real spiral wave. A convenient choice is that of an involute of a circle,

$$X = \rho_0 \cos(\sigma - \omega t) + \rho_0 \sigma \sin(\sigma - \omega t), \quad (2a)$$

$$Y = \rho_0 \sin(\sigma - \omega t) - \rho_0 \sigma \cos(\sigma - \omega t), \quad (2b)$$

parametrized by $\sigma = (\rho^2/\rho_0^2 - 1)^{1/2}$, where $\rho = |\mathbf{X}| = (X^2 + Y^2)^{1/2}$, and rotating with an angular velocity ω . The involute coordinate system (σ, r) is defined by the relation⁹

$$\mathbf{x} = \mathbf{X}(\sigma, t) + r\hat{\mathbf{f}}(\sigma), \quad (3)$$

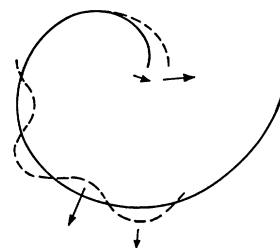


FIG. 1. Schematic illustration of the effect of curvature. Normal velocity (indicated by arrows) decreases as curvature increases. As a result small perturbations (dashed curves) that occur significantly far from the tip always decay, while those involving the tip may grow.

where $\hat{\mathbf{f}}$ is a unit vector normal to the spiral. The range of the normal coordinate r is chosen to be $(-d/2, d/2)$, where $d = 2\pi\rho_0$ is the pitch of the involute spiral. Figure 2 illustrates the notations.

The RDE's in the rotating involute frame become

$$\mathbf{L}\mathbf{U} + \mathbf{N}(\mathbf{U}) + D\partial_r^2\mathbf{U} + \omega\rho_0\partial_r\mathbf{U} = \mathbf{P}, \quad (4a)$$

$$\mathbf{P} = -DK_1\partial_r\mathbf{U} + \partial_t\mathbf{U} + \Omega\partial_\sigma\mathbf{U} - DK_1^2\partial_\sigma^2\mathbf{U}, \quad (4b)$$

where $K_1(\sigma, r) = K_0/(1+rK_0)$, $\Omega(\sigma, r) = \omega - \rho_0DK_1^3$, and $K_0(\sigma) = (\rho_0\sigma)^{-1}$ is the involute curvature. To avoid the singularity of K_0 at $\sigma=0$ we consider σ values larger than some lower bound σ_{\min} . The optimal choice of σ_{\min} is that which minimizes the perturbation \mathbf{P} . More specifically σ_{\min} is chosen such that $DK_1(\sigma_{\min}) \ll \omega\rho_0$ and all other terms in \mathbf{P} are at most of $O(DK_1)$.

Reaction-diffusion systems of the form of (1) but in one-dimensional space have been studied extensively.⁶ Solitary-wave solutions propagating with constant velocity have been found for specific realizations of the reaction part of (1).¹⁰ Let $\mathbf{H}(x - c_0t)$ be such a solution. Evidently \mathbf{H} solves the unperturbed part of (4) as well provided $c_0 = \omega\rho_0$. In fact it is a homoclinic orbit of that system biasymptotic to a saddle point representing the rest state of the medium. The asymptotic forms of the solitary-wave solution can be determined from a linear analysis around the saddle point. The dominant components of these forms are those eigenmodes whose eigenvalues have the largest negative and smallest positive real parts.

Extended patterns may conveniently be viewed as systems of many interacting localized structures. This approach has been used in the study of kink dynamics¹¹ and spatial chaos^{12,13} in one-dimensional systems, and will be used here to construct an approximate spiral solution. To this end the range of σ is split into segments $\sigma_{\min} + 2\pi(l-1) \leq \sigma_l < \sigma_{\min} + 2\pi l$ representing parallel portions of the spiral, as shown in Fig. 2. The localized structures to be used in this construction are solitary wave fronts that are peaked on these segments and solve the unperturbed problem: $\mathbf{H}_k(\sigma, r) \equiv \mathbf{H}(r + n(\sigma)d - kd)$,

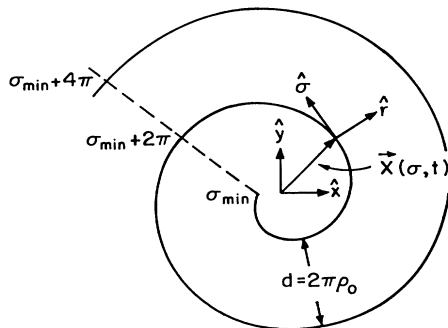


FIG. 2. The involute coordinate system (σ, r) . The position vector \mathbf{X} is given by Eqs. (2).

where $n(\sigma_l) \equiv l$. A general spiral solution is now written as a superposition of displaced solitary wave fronts:

$$\mathbf{U}(\sigma, r, t) = \sum_k \mathbf{H}_k(\sigma, r - \zeta_k) + \mathbf{R}(\sigma, r, t), \quad (5)$$

where \mathbf{R} is a correction term and the displacements $\zeta_k \equiv \zeta(\sigma_k, t)$ are evaluated at $\sigma_k = \sigma + 2\pi[k - n(\sigma)]$.

The form (5) should be understood as follows. Given a point (σ, r) in the plane, the main contribution to \mathbf{U} comes from the wave front that is peaked on $\sigma_{n(\sigma)}$: $\mathbf{H}(r - \zeta(\sigma, t))$. Next in order of importance are the contributions from the nearest neighbors, $\mathbf{H}(r \mp d - \zeta(\sigma \pm 2\pi, t))$, and so on. The condition $DK_1(\sigma_{\min}) \ll \omega\rho_0$ implies that the wave fronts are widely separated (large pitch). Consequently the correction term \mathbf{R} and its partial derivatives with respect to σ and time are expected to be small, and one may consider only nearest-neighbor interactions.

The geometrical form of the spiral wave is given by $\mathbf{x} = \mathbf{X}(\sigma, t) + \zeta(\sigma, t)\hat{\mathbf{f}}(\sigma, t)$, and our next objective is to derive partial differential equations for the displacements ζ_l . Upon introducing (5) into (4) one gets to leading order

$$\begin{aligned} \mathcal{L}_l\mathbf{R} = & \sum_k \mathbf{N}(\mathbf{H}_k) - \mathbf{N}\left(\sum_k \mathbf{H}_k\right) \\ & - (\partial_t\zeta_l + DK_1 + \Omega\partial_\sigma\zeta_l - DK_1^2\partial_\sigma^2\zeta_l)\mathbf{H}_l', \end{aligned} \quad (6)$$

where

$$\mathcal{L}_l \equiv \mathbf{L} + \nabla\mathbf{N}(\mathbf{H}_l) + D\partial_r^2 + \omega\rho_0\partial_r, \quad (7)$$

$\mathbf{H}_k = \mathbf{H}_k(\sigma, r - \zeta_k)$, and the prime denotes differentiation with respect to the second argument. The operator \mathcal{L}_l has a null vector (or zero mode), \mathbf{H}_l' . This is a consequence of the translational invariance of (1). Let \mathbf{G}_l be a null vector of the adjoint operator \mathcal{L}_l^\dagger where the inner product is defined to be

$$(\mathbf{f}, \mathbf{g}) = \sum_{i, n(\sigma)} \int_{-d/2}^{d/2} dr f_i[n(\sigma), r] g_i[n(\sigma), r].$$

The condition that the right-hand side of (6) is orthogonal to \mathbf{G}_l results in the dynamical equation

$$\begin{aligned} \partial_t\zeta_l = & -DK_{1,l} - \Omega_l\partial_\sigma\zeta_l + DK_{1,l}^2\partial_\sigma^2\zeta_l \\ & + F_L(\zeta_{l+1} - \zeta_l + d) + F_R(\zeta_l - \zeta_{l-1} + d), \end{aligned} \quad (8)$$

where $K_{1,l} \equiv K_1(\sigma_l, \zeta_l)$, $\Omega_l \equiv \Omega(\sigma_l, \zeta_l)$, and F_L and F_R are, respectively, the dominant components of the left- and right-hand asymptotic forms of \mathbf{H} . In deriving (8) use has been made of the localized nature of $\mathbf{H}(x)$ and $\mathbf{G}(x)$ around $x=0$.

The nonlocal terms F_R and F_L in (8) represent, respectively, the interactions of a given wave front with those behind and ahead of it. The functional forms of these terms are in general exponential for they follow from a linear analysis of the unperturbed problem around the quiescent state $\mathbf{U} = \mathbf{0}$. I will consider here solitary wave fronts with monotonic heads, $F_R(x)$

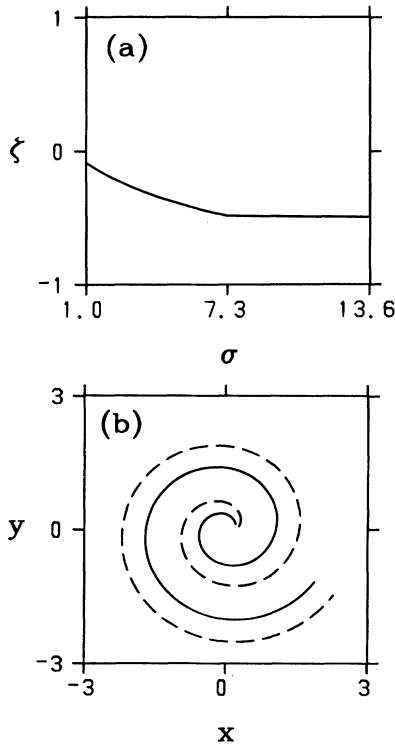


FIG. 3. (a) Asymptotic profile of ζ obtained by numerical integration of (8). Parameter values used are $\rho_0=0.2$, $\sigma_{min}=1.0$, $\omega=0.7$, $D=0.002$, $a_R=-a_L=1.0$, $\eta_R=10.0$, $\eta_L=3.0$, and $v_L=\phi_L=0.0$. (b) Asymptotic spiral (solid curve) and involute spiral (dashed curve) for the parameters of (a).

$=a_R \exp(-\eta_R x)$, but will allow for monotonic as well as oscillatory tails:

$$F_L(x) = a_L \exp(-\eta_L x) \cos(v_L x + \phi_L).$$

The eigenvalues η_R and $\eta_L \pm i v_L$ follow from the solitary-wave profile. The coefficients a_R and a_L require, in addition, the evaluation of certain integrals which are not displayed here.

A system (8) consisting of two wave fronts has been integrated numerically using the Crank-Nicholson scheme. The exponents $\eta_{R,L}$ and the coefficients $a_{R,L}$ were chosen to simulate conditions that are frequently met in chemical and biological applications: $\eta_L \ll \eta_R$, $a_L < 0$, and $a_R > 0$. In a considerably wide range of parameters, and for monotonic tails, $\zeta(\sigma, t)$ evolves toward a stationary profile $\zeta(\sigma)$, a typical form of which is displayed in Fig. 3(a). The corresponding spiral wave is shown in Fig. 3(b). The dashed curve is the involute coordinate system. The real spiral differs significantly from the involute only in the vicinity of the spiral core.

The dynamics of the spiral tip is illustrated in Fig. 4(a). The convergence to a stationary ζ profile in the case of monotonic tails implies a *stable* circular motion of the spiral tip (solid curve). The radius of circulation

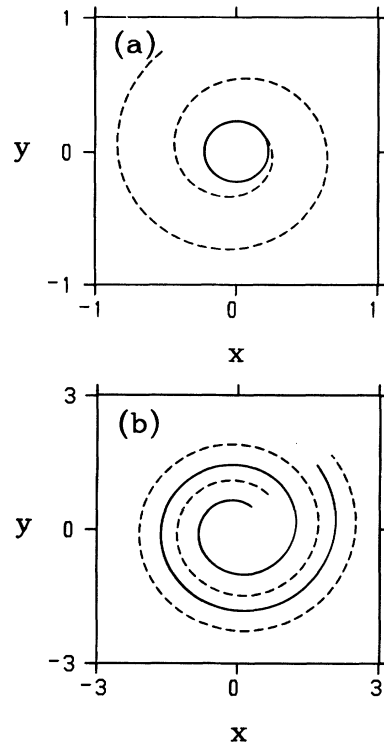


FIG. 4. (a) Dynamics of spiral tips. Steady circular motion obtained with a monotonic tail (solid curve) vs an outward spiral motion obtained with an oscillatory tail (dashed curve). Parameter values are as in Fig. 3 except that $v_L=2.0$ in the latter case. (b) Demonstration of core expansion. Spiral wave at an early stage (solid curve) and at a later time with larger core (dashed curve). Parameter values are as in Fig. 3 except that $v_L=2.0$.

is found to increase monotonically with η_L , the rate at which the wave front tails off, when ω and all other parameters are held constant. This monotonic growth terminates at a point at which the circular motion becomes unstable and noncircular tip dynamics set in. A complete account of the latter, commonly referred to as "tip meandering,"^{4,7,14} is postponed to a future work as it requires additional considerations (see discussion below).

When the nonlocal terms in (8) are removed no circular motion is observed; the spiral core typically expands. This observation is consistent with the heuristic argument for the destabilizing role of curvature and emphasizes the importance of nonlocal effects in stabilizing the dynamics of spiral waves. Core expansion may possibly be a real phenomenon when the tails are oscillatory.¹⁵ In that case the wave front that contains the tip tends to lock at a fixed distance from the wave front ahead of it, a distance that corresponds to one of the maxima of the oscillatory tail (or minima of threshold of excitation⁸). As a result the gradient of normal velocity in the vicinity of the tip becomes ever flatter and the ten-

dency to curl, ever weaker. The spiral tip therefore undergoes an outward spiral motion depicted in Fig. 4(a) by the dashed curve. The phenomenon is further illustrated in Fig. 4(b) where two forms of the spiral wave at different instants are shown. An interesting consequence of this result, which may bear on the problem of cardiac arrhythmias,⁴ is the possible elimination of spiral waves in finite systems. Experiments aimed at testing core expansion should be easier to conduct in chemical systems.^{1,2} Oscillatory tails are expected to appear in parameter range that precedes the bifurcation point to uniform oscillations.

Equation (8) can be used to derive an expression for the normal velocity of the spiral wave front, $v_r = \dot{\mathbf{x}} \cdot \hat{\mathbf{f}} = (\partial_t \mathbf{x} + \omega \partial_\sigma \mathbf{x}) \cdot \hat{\mathbf{f}}$, where $\mathbf{x} = \mathbf{X}(\sigma, t) + \zeta(\sigma, t) \hat{\mathbf{f}}(\sigma, t)$. Expressed in terms of the spiral-wave curvature,

$$K(\sigma, t) = (x_\sigma y_{\sigma\sigma} - y_\sigma x_{\sigma\sigma}) / (x_\sigma^2 + y_\sigma^2)^{3/2},$$

the normal velocity reads

$$v_r(\sigma_l, t) = \omega \rho_0 + F_L(\zeta_{l+1} - \zeta_l + d) + F_R(\zeta_l - \zeta_{l-1} + d) - DK(\sigma_l, t). \quad (9)$$

In the asymptotic regime where $\zeta(\sigma, t)$ attains a stationary profile, Eq. (9) admits the familiar form $v_r = c(\sigma) - DK(\sigma)$,⁶ where $c(\sigma)$, an undetermined function in previous studies, is given by the first three terms on the right-hand side of (9). At large σ values, for which curvature effects are negligible, the expression for c reduces to the dispersion relation of uniformly spaced wave trains of impulses.¹⁴

The present theory is still incomplete in so far as the dynamics of the spiral tip is concerned. The tip is a localized structure in a two-dimensional space, but only the structure along the normal coordinate has explicitly been considered. As a result only one degree of freedom,

$\zeta(\sigma_{\min}, t)$, describes the motion of the tip in the rotating frame. In order to allow for unconstrained tip dynamics a tangential degree of freedom should be introduced as well. Work in that direction is in progress.

The support of the United States-Israel Binational Science Foundation under Grant No. 86-0032 is gratefully acknowledged.

¹S. C. Muller, T. Plesser, and B. Hess, *Physica* (Amsterdam) **24D**, 71 (1987); **24D**, 87 (1987).

²W. Y. Tam, W. Horsthemke, Z. Noszticzius, and H. L. Swinney, *J. Chem. Phys.* **88**, 3395 (1988).

³R. J. Field and M. Burger, *Oscillations and Traveling Waves in Chemical Systems* (Wiley, New York, 1985).

⁴A. T. Winfree, *When Time Breaks Down* (Princeton Univ. Press, Princeton, NJ, 1987), and references therein.

⁵A. T. Winfree, *Science* **175**, 634 (1972).

⁶For a most recent review of previous theoretical works, see J. J. Tyson and J. P. Keener, *Physica* (Amsterdam) **32D**, 327 (1988).

⁷Wave-front interactions have been recently considered in a phenomenological way by V. S. Zykov, *Biophysics* **32**, 365 (1987).

⁸E. Meron and P. Pelcé, *Phys. Rev. Lett.* **60**, 1880 (1988).

⁹J. P. Keener, *SIAM J. Appl. Math.* **39**, 528 (1980).

¹⁰S. P. Hastings, *SIAM J. Appl. Math.* **42**, 247 (1982).

¹¹K. Kawasaki and T. Ohta, *Physica* (Amsterdam) **116A**, 573 (1982).

¹²P. Couillet, C. Elphick, and D. Repaux, *Phys. Rev. Lett.* **58**, 431 (1987).

¹³C. Elphick, E. Meron, and E. A. Spiegel, *Phys. Rev. Lett.* **61**, 496 (1988).

¹⁴V. S. Zykov, *Biophysics* **31**, 940 (1986).

¹⁵R. N. Miller and J. Rinzel, *Biophys. J.* **34**, 227 (1981); J. Rinzel and K. Maginu, in *Non-Equilibrium Dynamics in Chemical Systems*, edited by C. Vidal and A. Pacault (Springer-Verlag, Berlin, 1984).